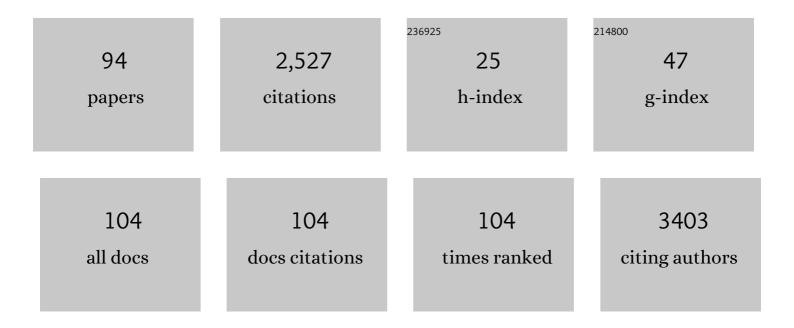
List of Publications by Year in descending order

Source: https://exaly.com/author-pdf/2323755/publications.pdf Version: 2024-02-01



Οινι Μλανιά

#	Article	IF	CITATIONS
1	Distinct skin morphological and transcriptomic profiles between wild and albino Oscar Astronotus ocellatus. Comparative Biochemistry and Physiology Part D: Genomics and Proteomics, 2022, 41, 100944.	1.0	2
2	Astragaloside IV suppresses migration and invasion of TGF.β1-induced human hepatoma HuH-7 cells by regulating Nrf2/HO-1 and TGF-I²1/Smad3 pathways. Naunyn-Schmiedeberg's Archives of Pharmacology, 2022, 395, 397-405.	3.0	7
3	Characterization of novel Tn7-derivatives and Tn7-like transposon found in Proteus mirabilis of food-producing animal origin in China. Journal of Global Antimicrobial Resistance, 2022, , .	2.2	3
4	Genome-wide identification and expression pattern analysis of novel chemosensory genes in the German cockroach Blattella germanica. Genomics, 2022, 114, 110310.	2.9	5
5	Spatiotemporal Investigation of Near-Surface CO ₂ and Its Affecting Factors Over Asia. IEEE Transactions on Geoscience and Remote Sensing, 2022, 60, 1-16.	6.3	9
6	A Racemic Naphthyl oumarinâ€Based Probe for Quantitative Enantiomeric Excess Analysis of Amino Acids and Enantioselective Sensing of Amines and Amino Alcohols. ChemistryOpen, 2022, 11, .	1.9	2
7	Ghrelin ameliorates nonalcoholic steatohepatitis induced by chronic lowâ€grade inflammation via blockade of Kupffer cellÂM1 polarization. Journal of Cellular Physiology, 2021, 236, 5121-5133.	4.1	20
8	Nocturnal Systolic Hypertension and Adverse Prognosis in Patients with CKD. Clinical Journal of the American Society of Nephrology: CJASN, 2021, 16, 356-364.	4.5	9
9	Validation of GOSAT and OCO-2 against In Situ Aircraft Measurements and Comparison with CarbonTracker and GEOS-Chem over Qinhuangdao, China. Remote Sensing, 2021, 13, 899.	4.0	22
10	Smad3 gene C-terminal phosphorylation site mutation exacerbates CCl4-induced hepatic fibrogenesis by promoting pSmad2L/C-mediated signaling transduction. Naunyn-Schmiedeberg's Archives of Pharmacology, 2021, 394, 1779-1786.	3.0	1
11	CircSPAG16 suppresses cadmiumâ€induced transformation of human bronchial epithelial cells by decoying PIP5K1α to inactivate Akt. Molecular Carcinogenesis, 2021, 60, 582-594.	2.7	4
12	A novel circular RNA, circPUS7 promotes cadmium-induced transformation of human bronchial epithelial cells by regulating Kirsten rat sarcoma viral oncogene homolog expression via sponging miR-770. Metallomics, 2021, 13, .	2.4	3
13	Synthesis and Biological Evaluation of Falcarinol-Type Analogues as Potential Calcium Channel Blockers. Journal of Natural Products, 2021, 84, 2138-2148.	3.0	1
14	Synthesis, Anticancer Activity, Structureâ€Activity Relationship and Mechanistic Investigations of Falcarindiol Analogues. ChemMedChem, 2021, 16, 3569-3575.	3.2	2
15	Comparative Analyses of the Transcriptome and Proteome of Escherichia coli C321.â– ³ A and Further Improving Its Noncanonical Amino Acids Containing Protein Expression Ability by Integration of T7 RNA Polymerase. Frontiers in Microbiology, 2021, 12, 744284.	3.5	5
16	Astragaloside IV inhibits hepatocellular carcinoma by continually suppressing the development of fibrosis and regulating pSmad3C/3L and Nrf2/HO-1 pathways. Journal of Ethnopharmacology, 2021, 279, 114350.	4.1	24
17	ALKBH5 promotes cadmium-induced transformation of human bronchial epithelial cells by regulating PTEN expression in an m6A-dependent manner. Ecotoxicology and Environmental Safety, 2021, 224, 112686.	6.0	13
18	A crystalline covalent organic framework embedded with a crystalline supramolecular organic framework for efficient iodine capture. Journal of Materials Chemistry A, 2021, 9, 16961-16966.	10.3	43

#	Article	IF	CITATIONS
19	Enhancement of Activity and Thermostability of Keratinase From Pseudomonas aeruginosa CCTCC AB2013184 by Directed Evolution With Noncanonical Amino Acids. Frontiers in Bioengineering and Biotechnology, 2021, 9, 770907.	4.1	9
20	Effects of Nisin, Cecropin, and Penthorum chinense Pursh on the Intestinal Microbiome of Common Carp (Cyprinus carpio). Frontiers in Nutrition, 2021, 8, 729437.	3.7	17
21	Utilization of antihypertensive drugs among chronic kidney disease patients: Results from the Chinese cohort study of chronic kidney disease (C‧TRIDE). Journal of Clinical Hypertension, 2020, 22, 57-64.	2.0	4
22	Selective detection of Cys and GSH by using one fluorescent probe at two excitation wavelengths. Tetrahedron Letters, 2020, 61, 152462.	1.4	3
23	Characterization of a thermostable phytase from Bacillus licheniformis WHU and further stabilization of the enzyme through disulfide bond engineering. Enzyme and Microbial Technology, 2020, 142, 109679.	3.2	15
24	Highly Diastereoselective Synthesis of 2,2-Disubstituted Cyclopentane-1,3-diols via Stepwise Ketone Reduction Enabling Concise Chirality Construction. Journal of Organic Chemistry, 2020, 85, 9599-9606.	3.2	4
25	Multi-Year Comparison of CO2 Concentration from NOAA Carbon Tracker Reanalysis Model with Data from GOSAT and OCO-2 over Asia. Remote Sensing, 2020, 12, 2498.	4.0	27
26	Enhancement of keratin-degradation ability of the keratinase KerBL from Bacillus licheniformis WHU by proximity-triggered chemical crosslinking. International Journal of Biological Macromolecules, 2020, 163, 1458-1470.	7.5	12
27	Structure of a Dimeric BINOL-Imine-Zn(II) Complex and Its Role in Enantioselective Fluorescent Recognition. Inorganic Chemistry, 2020, 59, 17992-17998.	4.0	11
28	PLA ₂ -Triggered Release of Drugs from Self-Assembled Lipid Tubules for Arthritis Treatments. ACS Applied Bio Materials, 2020, 3, 6488-6496.	4.6	12
29	Comparative analysis of the gut microbiota of grass carp fed with chicken faeces. Environmental Science and Pollution Research, 2020, 27, 32888-32898.	5.3	11
30	White-coat hypertension and incident end-stage renal disease in patients with non-dialysis chronic kidney disease: results from the C-STRIDE Study. Journal of Translational Medicine, 2020, 18, 238.	4.4	7
31	Insight Into the Effects of Nisin and Cecropin on the Oral Microbial Community of Rats by High-Throughput Sequencing. Frontiers in Microbiology, 2020, 11, 1082.	3.5	9
32	Synergistic enhancement of cytotoxicity against cancer cells by incorporation of rectorite into the paclitaxel immobilized cellulose acetate nanofibers. International Journal of Biological Macromolecules, 2020, 152, 672-680.	7.5	19
33	Mechanistic Study on a BINOL–Coumarin-Based Probe for Enantioselective Fluorescent Recognition of Amino Acids. Journal of Organic Chemistry, 2020, 85, 6352-6358.	3.2	16
34	Construction of functional chimeras of syntaxin-1A and its yeast orthologue, and their application to the yeast cell-based assay for botulinum neurotoxin serotype C. Biochimica Et Biophysica Acta - General Subjects, 2019, 1863, 129396.	2.4	2
35	Assessing the development and treatment of rheumatoid arthritis using multiparametric photoacoustic and ultrasound imaging. Journal of Biophotonics, 2019, 12, e201900127.	2.3	18
36	Enhanced Activity and Substrate Specificity by Siteâ€Directed Mutagenesis for the P450 119 Peroxygenase Catalyzed Sulfoxidation of Thioanisole. ChemistryOpen, 2019, 8, 1076-1083.	1.9	6

#	Article	IF	CITATIONS
37	Excitation of One Fluorescent Probe at Two Different Wavelengths to Determine the Concentration and Enantiomeric Composition of Amino Acids. Organic Letters, 2019, 21, 9036-9039.	4.6	14
38	Preparation of pyrido[1,2-c][1,2,4]triazole-based π-conjugated triazene as a Fe3+ ion fluorescent sensor. Chinese Chemical Letters, 2019, 30, 1059-1062.	9.0	9
39	Biogenic iron mineralization of polyferric sulfate by dissimilatory iron reducing bacteria: Effects of medium composition and electric field stimulation. Science of the Total Environment, 2019, 684, 466-475.	8.0	14
40	Liposome mediated-CYP1A1 gene silencing nanomedicine prepared using lipid film-coated proliposomes as a potential treatment strategy of lung cancer. International Journal of Pharmaceutics, 2019, 566, 185-193.	5.2	16
41	Dynamic Mapping and Quality of Service Driven Re-Embedding in Virtualization Environment. , 2019, , .		7
42	Sirtuin 6 inhibits myofibroblast differentiation via inactivating transforming growth factorâ€Î²1/Smad2 and nuclear factorâ€iºB signaling pathways in human fetal lung fibroblasts. Journal of Cellular Biochemistry, 2019, 120, 93-104.	2.6	41
43	Optimized in vivo performance of acid-liable micelles for the treatment of rheumatoid arthritis by one single injection. Nano Research, 2019, 12, 421-428.	10.4	24
44	Fluoride induces apoptosis via inhibiting SIRT1 activity to activate mitochondrial p53 pathway in human neuroblastoma SH-SY5Y cells. Toxicology and Applied Pharmacology, 2018, 347, 60-69.	2.8	58
45	Enhanced Turnover for the P450 119 Peroxygenaseâ€Catalyzed Asymmetric Epoxidation of Styrenes by Random Mutagenesis. Chemistry - A European Journal, 2018, 24, 2741-2749.	3.3	16
46	Ghrelin Restores the Disruption of the Circadian Clock in Steatotic Liver. International Journal of Molecular Sciences, 2018, 19, 3134.	4.1	30
47	<i>O</i> â€Alkylation of 3â€Formylâ€BINOL and Its Strong Effect on the Fluorescence Recognition of 1,3â€Diaminopropane. European Journal of Organic Chemistry, 2018, 2018, 4972-4977.	2.4	9
48	Rationally Designed Selfâ€Assembling Nanoparticles to Overcome Mucus and Epithelium Transport Barriers for Oral Vaccines against <i>Helicobacter pylori</i> . Advanced Functional Materials, 2018, 28, 1802675.	14.9	37
49	Combining photothermal therapy and immunotherapy against melanoma by polydopamine-coated Al ₂ O ₃ nanoparticles. Theranostics, 2018, 8, 2229-2241.	10.0	116
50	Highly Enantioselective Synthesis and Anticancer Activities of Chiral Conjugated Diynols. ChemBioChem, 2018, 19, 2293-2299.	2.6	6
51	Targeting NF-kB signaling with polymeric hybrid micelles that co-deliver siRNA and dexamethasone for arthritis therapy. Biomaterials, 2017, 122, 10-22.	11.4	161
52	Effects of temperature and pressure on the nucleation and growth of silver clusters from supersaturated vapor: A molecular dynamics analysis. International Journal of Modern Physics B, 2017, 31, 1750057.	2.0	3
53	Combined delivery of a TGF-β inhibitor and an adenoviral vector expressing interleukin-12 potentiates cancer immunotherapy. Acta Biomaterialia, 2017, 61, 114-123.	8.3	29
54	Recent advances in nanomedicines for the treatment of rheumatoid arthritis. Biomaterials Science, 2017, 5, 1407-1420.	5.4	100

QIN WANG

#	Article	IF	CITATIONS
55	Access to Fluorescent Azines from Nâ€Heterocyclic Carbene Precursors and <i>N</i> â€Tosylhydrazones. Advanced Synthesis and Catalysis, 2017, 359, 1825-1830.	4.3	5
56	pH-sensitive polymeric micelles for targeted delivery to inflamed joints. Journal of Controlled Release, 2017, 246, 133-141.	9.9	114
57	Lymph node targeting strategies to improve vaccination efficacy. Journal of Controlled Release, 2017, 267, 47-56.	9.9	207
58	Tissue factor pathway inhibitor-2 induced hepatocellular carcinoma cell differentiation. Saudi Journal of Biological Sciences, 2017, 24, 95-102.	3.8	14
59	Total Synthesis of Chiral Falcarindiol Analogues Using BINOL-Promoted Alkyne Addition to Aldehydes. Molecules, 2016, 21, 112.	3.8	7
60	Targeted delivery of low-dose dexamethasone using PCL–PEG micelles for effective treatment of rheumatoid arthritis. Journal of Controlled Release, 2016, 230, 64-72.	9.9	171
61	Highly enantioselective catalytic methyl propiolate addition to both aromatic and aliphatic aldehydes. Tetrahedron: Asymmetry, 2016, 27, 428-435.	1.8	6
62	HPLC Determination of Enantiomeric Purity for 1-Styrene-3-Hexyl Propynol. Journal of Chromatographic Science, 2016, 54, 1794-1799.	1.4	0
63	Engineering P450 Peroxygenase to Catalyze Highly Enantioselective Epoxidation of <i>cis</i> â€î²â€Methylstyrenes. Chemistry - A European Journal, 2016, 22, 10969-10975.	3.3	21
64	Enzyme-assisted cycling amplification and DNA-templated in-situ deposition of silver nanoparticles for the sensitive electrochemical detection of Hg2+. Biosensors and Bioelectronics, 2016, 86, 630-635.	10.1	36
65	An amplified electrochemical proximity immunoassay for the total protein of Nosema bombycis based on the catalytic activity of Fe3O4NPs towards methylene blue. Biosensors and Bioelectronics, 2016, 81, 382-387.	10.1	25
66	A Prime–Boost Strategy Combining Intravaginal and Intramuscular Administration of Homologous Adenovirus to Enhance Immune Response Against HIV-1 in Mice. Human Gene Therapy, 2016, 27, 219-229.	2.7	3
67	Efficient entanglement concentration for concatenated Greenberger–Horne–Zeilinger state with the cross-Kerr nonlinearity. Quantum Information Processing, 2016, 15, 1669-1687.	2.2	31
68	Bio-inspired polymer envelopes around adenoviral vectors to reduce immunogenicity and improve in vivo kinetics. Acta Biomaterialia, 2016, 30, 94-105.	8.3	28
69	Blood pressure and renal function decline. Journal of Hypertension, 2015, 33, 136-143.	0.5	17
70	Transcriptome sequencing and differential gene expression analysis in Viola yedoensis Makino (Fam.) Tj ETQqO Communications, 2015, 459, 60-65.	0 0 rgBT /C 2.1	Overlock 10 Th 26
71	Use of partial least-squares discriminant analysis to study the effects of gradual scale-up of culture, and optimization of bioreactor angle and aeration volume on culture of Panax quinquefolium L. adventitious roots in a 5-L balloon-type bubble bioreactor. Research on Chemical Intermediates, 2015,	2.7	0
72	41, 6707-6720. Influence of step-wise aeration treatment on biomass and bioactive compounds of Panax ginseng adventitious root in balloon-type bubble bioreactor. Research on Chemical Intermediates, 2015, 41,	2.7	3

adventitious root in balloon-type bubble bioreactor. Research on Chemical Intermediates, 2015, 41, 623-629. 72

#	Article	IF	CITATIONS
73	Optimization of balloon-type bubble bioreactor angle and methyl jasmonate concentration to enhance metabolite production in adventitious roots of Pseudostellaria heterophylla. Research on Chemical Intermediates, 2015, 41, 5555-5563.	2.7	4
74	Associations between Serum-Intact Parathyroid Hormone, Serum 25-Hydroxyvitamin D. Oral Vitamin D Analogs and Metabolic Syndrome in Peritoneal Dialysis Patients: A Multi-Center Cross-Sectional Study. Peritoneal Dialysis International, 2014, 34, 447-455.	2.3	12
75	Optimization and quality assessment of adventitious roots culture in Panax quinquefolium L Acta Physiologiae Plantarum, 2014, 36, 713-719.	2.1	19
76	Reinforcement of phenylalanine-based supramolecular hydrogels by hybridizing poly(N-isopropylacrylamide) nanogels. RSC Advances, 2014, 4, 22380-22386.	3.6	5
77	Enhanced turnover rate and enantioselectivity in the asymmetric epoxidation of styrene by new T213G mutants of CYP 119. RSC Advances, 2014, 4, 27526-27531.	3.6	15
78	Reinforced conducting hydrogels prepared from the in situ polymerization of aniline in an aqueous solution of sodium alginate. Journal of Materials Chemistry A, 2014, 2, 16516-16522.	10.3	93
79	Electrochemical immunosensor for detecting the spore wall protein of Nosema bombycis based on the amplification of hemin/G-quadruplex DNAzyme concatamers functionalized Pt@Pd nanowires. Biosensors and Bioelectronics, 2014, 60, 118-123.	10.1	47
80	Diverse Transformations of Chiral Propargylic Alcohols Generated by BINOL-Catalyzed Alkyne Addition to Aldehydes. Synlett, 2013, 24, 1340-1363.	1.8	23
81	Highly enantioselective addition of linear alkyl alkynes to aromatic aldehydes. Tetrahedron: Asymmetry, 2011, 22, 1142-1146.	1.8	15
82	Directed evolution of Streptomyces lividans xylanase B toward enhanced thermal and alkaline pH stability. World Journal of Microbiology and Biotechnology, 2009, 25, 93-100.	3.6	15
83	Kinetics and Activation Parameters for Oxidations of Styrene by Compounds I from the Cytochrome P450 _{BM-3} (CYP102A1) Heme Domain and from CYP119. Biochemistry, 2009, 48, 9140-9146.	2.5	25
84	Quantitative Production of Compound I from a Cytochrome P450 Enzyme at Low Temperatures. Kinetics, Activation Parameters, and Kinetic Isotope Effects for Oxidation of Benzyl Alcohol. Journal of the American Chemical Society, 2009, 131, 10629-10636.	13.7	58
85	Highly Reactive Porphyrinâ^'Ironâ^'Oxo Derivatives Produced by Photolyses of Metastable Porphyrinâ^'Iron(IV) Diperchlorates. Journal of the American Chemical Society, 2009, 131, 2621-2628.	13.7	71
86	Asymmetric synthesis of 2,6-substituted dihydropyrone catalyzed by 3-monosubstituted and 3,3′-bisubstituted BINOL titanium complexes. Chemical Papers, 2008, 62, .	2.2	2
87	Copper-catalyzed cleavage of benzyl ethers with (diacetoxyiodo)- benzene and p-toluenesulfonamide. Arkivoc, 2008, 2008, 103-108.	0.5	2
88	Enantioselective Fluorescent Recognition of Amino Alcohols by a Chiral Tetrahydroxyl 1,1â€ [~] -Binaphthyl Compound. Journal of Organic Chemistry, 2007, 72, 97-101.	3.2	82
89	1,1′-Binaphthyl ligands with bulky 3,3′-tertiaryalkyl substituents for the asymmetric alkyne addition to aromatic aldehydes. Tetrahedron, 2007, 63, 4422-4428.	1.9	22
90	Synthesis and copolymerization of pentachlorophenyl acrylate monomers. Arkivoc, 2007, 2006, 75-82.	0.5	0

QIN WANG

#	Article	IF	CITATIONS
91	Monometallic complexes of 1,4,7,10-tetraazacyclododecane containing an imidazolium side: Synthesis, characterization, and their interaction with plasmid DNA. Bioorganic and Medicinal Chemistry, 2006, 14, 4151-4157.	3.0	79
92	Highly Enantioselective Synthesis of γ-Hydroxy-α,β-acetylenic Esters by Asymmetric Alkyne Addition to Aldehydes. Angewandte Chemie - International Edition, 2006, 45, 122-125.	13.8	111
93	UNIFORM EMBEDDINGS OF FREE PRODUCTS INTO UNIFORMLY CONVEX BANACH SPACES. Bulletin of the London Mathematical Society, 2006, 38, 139-142.	0.8	Ο
94	Synthesis of small cyclic peptides containing disulfide bonds. Arkivoc, 2006, 2006, 148-154.	0.5	11